



## Understanding nitrate formation in a world with less sulfate.

1

Petros Vasilakos<sup>1</sup>, Armistead Russell<sup>2</sup>, Rodney Weber<sup>3</sup>, and Athanasios Nenes<sup>1,3,4,5†</sup>

<sup>1</sup>School of Chemical and Biomolecular Engineering, Georgia Institute of Technology, Atlanta, Georgia, 30332, USA

<sup>2</sup>School of Civil and Environmental Engineering, Georgia Institute of Technology, Atlanta, Georgia, 30332, USA

<sup>3</sup>School of Earth and Atmospheric Sciences, Georgia Institute of Technology, Atlanta, Georgia, 30332, USA

<sup>4</sup>Institute of Chemical Engineering Sciences, Foundation for Research and Technology-Hellas, Patras, GR 26504, Greece

<sup>5</sup>Institute for Environmental Research and Sustainable Development, National Observatory of Athens, Palea Penteli, GR 15236, Greece

†Corresponding Author: A. Nenes ([athanasios.nenes@gatech.edu](mailto:athanasios.nenes@gatech.edu))

2



## Abstract

3           SO<sub>2</sub> emission controls, combined with modestly increasing ammonia, have been thought  
4 to generate aerosol of significantly reduced acidity where sulfate is partially substituted by nitrate.  
5 However, neither expectation agrees with decadal observations in the Southeastern US, suggesting  
6 that a fundamentally different response of aerosol pH to emissions changes is occurring. We  
7 postulate this “nitrate substitution paradox” arises from a positive bias in aerosol pH in model  
8 simulations, exacerbated by reductions in SO<sub>2</sub> emissions. This bias can elevate pH to where nitrate  
9 partitioning is readily promoted, leading to behavior consistent with “nitrate substitution”. CMAQ  
10 simulations are used to investigate this hypothesis; predictions of PM<sub>2.5</sub> pH for 2001 emissions  
11 compare favorably with observations; for 2011 emissions however, predicted pH increases by 1  
12 unit, presenting a positive trend not seen in the observations. Non-volatile cations (K<sup>+</sup>, Na<sup>+</sup>, Ca<sup>+2</sup>  
13 and Mg<sup>+2</sup>) in the fine mode are found responsible for most of this trend. pH biases of 1 unit can  
14 induce a nitrate bias of 1-2 μg m<sup>-3</sup> which may further increase in future projections, reaffirming  
15 an otherwise incorrect expectation of “nitrate substitution”. Evaluation of predicted aerosol pH  
16 against thermodynamic analysis of observations is therefore a critically important, but overlooked,  
17 aspect of model evaluation for robust emissions policy.

18



## 19 Introduction

20 Aerosol acidity is a driver of many important atmospheric processes (Guo et al. 2015,  
21 Weber et al. 2016), catalyzing the conversion of isoprene oxidation products to form secondary  
22 organic aerosol (SOA) (Xu et al. 2015, Pye et al. 2013, Surrat et al. 2010, Eddingsaas et al. 2010),  
23 driving the semi-volatile partitioning of key aerosol species processes (Guo et al. 2015, Weber et  
24 al. 2016), as well as the solubilization of iron, copper and other trace metals in aerosol which may  
25 serve as nutrients for ecosystems (Meskhidze et al. 2003), but also prove toxic for humans (Ghio  
26 et al. 2012, Fang et al. 2017). Significant reductions in primary pollutant emissions over the last  
27 decades has greatly improved air quality in the developed world, and is also thought to  
28 fundamentally affect aerosol acidity. SO<sub>2</sub>, an important aerosol precursor and a major driver of its  
29 acidity, has seen decreases of about 6% yr<sup>-1</sup> over the 2001-2011 period alone in the US, with a  
30 continued anticipated downward trend (West et al. 1999, Pinder et al. 2007, 2008). Emissions of  
31 NO<sub>x</sub> and the resulting acidic HNO<sub>3</sub>, are also declining. In contrast, ammonia, the primary alkaline  
32 fine mode aerosol precursor, is either constant or increasing (Pinder et al. 2007, 2008, Heald et al.  
33 2012), owing to intensified agricultural activity and livestock farming from the demands of  
34 population growth. These trends have created the expectation that the aerosol has and will become  
35 increasingly neutralized (West et al. 1999, Pinder et al. 2007, 2008, Heald et al. 2012, Tsimpidi et  
36 al. 2007, Saylor et al. 2015), with ammonium sulfate being replaced, at least in part, by ammonium  
37 nitrate (West et al. 1999, Bauer et al. 2007, Bellouin et al. 2007, Li et al. 2014, Goto et al. 2016).

38 The concept of “nitrate substitution” of sulfate has largely been based on the notion that  
39 nitrate is volatile when the aerosol is acidic, and in turn aerosol is acidic when insufficient amounts  
40 of total ammonia (i.e., gas+aerosol) or dust non-volatile cations (NVCs) exist to neutralize aerosol  
41 sulfate. Based on this conceptual model, aerosol ionic molar ratios have largely been used as  
42 proxies of aerosol acidity (pH), so that when the aerosol ammonium to sulfate molar ratio  
43 approaches 2 (the composition of ammonium sulfate), aerosol is assumed “neutral” and only then  
44 nitrate aerosol can form (Fisher et al. 2011, Hennigan et al. 2015, Wang et al. 2016, Silvern et al.  
45 2017). Modeling studies have corroborated this view, predicting that nitrate substitution may be  
46 prevalent in the future, including the Southeastern US (SE US) (Heald et al. 2014, Baur et al.  
47 2007, Bellouin et al. 2011, Li et al. 2014, Goto et al. 2016, Vayenas et al. 2005, Karydis et al.  
48 2016). A more careful analysis however (Guo et al. 2015, Weber et al. 2016, Hennigan et al. 2015,  
49 Guo et al. 2016) reveals that this conceptual model of aerosol acidity and conditions for nitrate



50 substitution fail; thermodynamic analysis of SE US aerosol observations instead show that fine  
51 mode aerosol remains strongly acidic, despite a 70% reduction in sulfates, and more than sufficient  
52 total ammonia to neutralize it. The strong acidity is maintained by the large difference in volatility  
53 between sulfate and ammonia (Guo et al. 2015, Weber et al. 2016), so large changes in total  
54 ammonia concentrations are required for a notable change in aerosol acidity, about one order of  
55 magnitude increase in  $\text{NH}_3$  concentration per unit increase in aerosol pH (Guo et al. 2015 &  
56 2017a). However, ammonia gas deposits relatively rapidly, limiting its build up except in high  
57 emissions regions. Throughout the decade, the levels of aerosol nitrate have remained relatively  
58 constant throughout the US (Guo et al. 2015, Weber et al. 2016, Pye et al. 2009). The persistent  
59 strong aerosol acidity in turn explains why nitrate aerosol has not considerably increased over the  
60 last decades, and is unlikely to appear in the immediate future in the SE US. These findings  
61 constitute a “paradox”, as the same thermodynamic models (e.g., ISORROPIA-II Fountoukis &  
62 Nenes 2007) used to demonstrate the aerosol tendency for strong acidity in the SE US (Guo et al.  
63 2015, Weber et al. 2016) using ambient data, is also used in 3D modeling studies (Pye et al. 2009,  
64 Heald et al. 2012) for the region that predict nitrate substitution as a possible aerosol response.

65 Reconciling the “nitrate substitution paradox” requires a careful examination of aerosol  
66 thermodynamics and the conditions under which nitrate partitioning to the aerosol is favored.  
67 Meskhidze et al. (2003) and later Guo et al. (2016) showed that for aerosol nitrate formation to  
68 occur, aerosol pH needs to exceed a certain characteristic value (that depending on the temperature  
69 and the amount of liquid water, ranges between a pH of 1.5 and 3; Guo et al., 2017). If aerosol pH  
70 is therefore high enough (typically above a pH of 2.5 to 3), a behavior consistent with “nitrate  
71 substitution” emerges, because any inorganic nitrate forming from  $\text{NO}_x$  chemistry mostly resides  
72 in the aerosol phase. When pH is low enough (typically below 1.5 to 2), nitrate remains exclusively  
73 in the gas phase (as  $\text{HNO}_3$ ), regardless of the amount produced, and “nitrate substitution” is not  
74 observed. Between these “high” and “low” pH values, a “sensitivity window” emerges (of  
75 typically 1-1.5 pH units), where partitioning shifts from nitrate being predominantly found as gas  
76 to where it is mostly found as an aerosol. Therefore, if a model is for any reason biased in its  
77 prediction of aerosol pH, it may be preconditioned towards nitrate prediction biases. The  
78 sensitivity to pH biases is strongest when the aerosol lies in the pH “sensitivity window”, which  
79 is often the case for atmospheric aerosol (Guo et al. 2015, 2016 & 2017, Bougiatioti et al. 2016).  
80 When below this “pH sensitivity window”, aerosol nitrate is almost nonexistent and relatively



81 insensitive to emissions (and pH biases); when above the window, almost all nitrate resides in the  
82 aerosol phase, and directly responds to NO<sub>x</sub> emission controls.

83 If aerosol were composed only of non-volatile sulfate and semi-volatile nitrate and  
84 ammonium, prediction biases in pH could result only from errors in RH, and large errors (e.g.,  
85 order of magnitude) of NH<sub>3</sub>, NO<sub>x</sub> and SO<sub>2</sub> because pH is relatively insensitive to changes in these  
86 aerosol precursors (Hennigan et al. 2015). Acidity however can also be modulated by other soluble  
87 inorganic cations from seasalt and mineral dust, such as K<sup>+</sup>, Na<sup>+</sup>, Ca<sup>+2</sup> and Mg<sup>+2</sup>. The low volatility  
88 of these cations allows them to preferentially neutralize sulfates over NH<sub>3</sub>, and, even in small  
89 amounts elevate particle pH to levels that can promote the partitioning of nitrates to the aerosol  
90 phase (Fountoukis & Nenes 2007, Guo et al. 2017). NVCs tend to reside in the coarse mode aerosol  
91 (Guo et al. 2015, West et al. 1999, Vayenas et al. 2005), with a fraction found in smaller particles,  
92 while sulfate tends to reside in the fine mode (e.g., West et al. 1999, Vayenas et al. 2005, Guo et  
93 al. 2015); the degree to which NVCs can affect fine mode pH therefore lies in the degree to which  
94 the two types of species mix across different particle sizes. Potential interactions between  
95 inorganics-organics can also affect aerosol acidity. However, recent studies driving  
96 thermodynamic models utilizing water associated with organics find only minimal differences  
97 between predicted pH (Guo et al. 2015, Bougiatioti et al. 2016, Liu et al. 2017, Pye et al., 2018,  
98 Song et al. 2018). In the presence of very high NVCs (for example in sea-spray aerosol), where  
99 the aerosol has much higher pH, the pH can approach the pK<sub>a</sub> of organic acids, leading to  
100 conditions where their dissociation can contribute to aerosol acidity (Laskin et al. 2012).

101 Although aerosol models are evaluated in terms of their ability to predict the concentration  
102 of aerosol species (including across size), no studies to date focus on their ability to predict aerosol  
103 pH across size, even though it is known to potentially vary up to 6 units (Fang et al. 2017,  
104 Bougiatioti et al. 2016, Li et al. 2017). Evaluation of models in this context is challenging, since  
105 there is no established dataset of aerosol acidity - although that is rapidly changing, with pH  
106 estimates derived from a combination of observations and models (e.g., Guo et al., 2015;  
107 Bougiatioti et al., 2016; Guo et al., 2017; Liu et al., 2017; Song et al., 2018) -. Furthermore, given  
108 that most of this pH variability occurs in the PM<sub>1</sub> to PM<sub>2.5</sub> range (Fang et al. 2017), it is quite  
109 likely that model assumptions on how aerosol species interact within a mode (degree of internal  
110 mixture), especially for particles in the 1-2.5 μm range, may lead to pH prediction biases that drive  
111 model behavior.



112 This aim of this study is to address the underlying reasons for the “nitrate substitution”  
113 paradox, and in the process, provide a conceptual framework for quantifying and understanding  
114 the importance of aerosol pH biases. The guiding hypothesis of this work is that aerosol pH  
115 prediction bias fundamentally changes predicted aerosol behavior and the underlying cause of the  
116 paradox. The approach is demonstrated with the Community Multiscale Air Quality (CMAQ)  
117 model (Byun & Schere 2006) and is based on predictions of pH over the 2001-2011 period in the  
118 Southeastern/Eastern US, being the region for which aerosol pH trends are constrained by  
119 observations. The role of internally-mixed nonvolatile cations in  $PM_{2.5}$  as a source of the pH bias  
120 is then assessed.

121

## 122 **Methods**

### 123 **Predicting aerosol pH and composition**

124 CMAQ is a three-dimensional, Eulerian, atmospheric chemistry and transport model, that  
125 simulates the processes atmospherically relevant compounds undergo, such as emission, diffusion,  
126 chemical reactions and deposition (Byun & Schere 2006). CMAQ version 5.0.2 was used in this  
127 study, and simulations were carried out using a 36-km horizontal resolution grid, with 13 vertical  
128 layers, over the continental US (CONUS) for the entire years of 2001 & 2011. Meteorological  
129 data were obtained offline from the Weather Research Forecasting (WRF) model. The same  
130 meteorology was used between the two years to eliminate potential biases of temperature and  
131 relative humidity on pH predictions. Model-ready emissions for 2011 were obtained using the  
132 National Emissions Inventory 2011 inventory (NEI 2011) for the Carbon Bond 05 (CB05)  
133 chemical mechanism. To estimate the 2001 emissions, the 2011 emissions for  $SO_2$ ,  $NO_x$ ,  $NH_3$ ,  
134  $CO$ , VOCs and primary PM from anthropogenic sources were scaled on a per-species basis using  
135 the Air Pollutant Emissions Trends Data; emissions for other species were kept constant.  
136 Emissions of biogenic species were calculated online using the Biogenic Emission Inventory  
137 System (BEIS).

138 The aerosol thermodynamic model ISORROPIA-II (subversion 2.2 - dated 2012 –  
139 Fountoukis & Nenes 2007) was used online in CMAQ to drive the semivolatile partitioning of  
140 inorganic species, as well as offline to analyze the predicted  $PM_{2.5}$  pH, nitrate partitioning  
141 tendency and sensitivities thereof to nonvolatile cations. It should be noted that ISORROPIA and  
142 CMAQ only account for the thermodynamic interactions between inorganic species and do not



143 treat organics. Offline calculations were conducted using the hourly gas and particle phase  
144 concentrations output from CMAQ for the 2001 and 2011 simulations, which includes NVCs, and  
145 using them as input to ISORROPIA-II. The thermodynamic calculations online and offline were  
146 carried out in forward mode, meaning that the temperature, relative humidity, as well as all aerosol  
147 and gas phase concentrations were known and used as input, assuming that the aerosol is in a  
148 metastable state, where only one aqueous phase is allowed to exist (Fountoukis & Nenes 2007).  
149 This assumption is not always necessarily true, especially under conditions of low relative  
150 humidity ( $RH < 30\%$ ) where the aerosol can crystallize or exist in glassy, amorphous state (where  
151 in this case thermodynamic equilibrium is not reached), observational data of liquid water content  
152 shows that it is most often a valid assumption (Guo et al. 2015, Bougiatioti et al. 2016), and other  
153 studies suggest that the phase state may not strongly affect predicted pH (Song et al., 2018). We  
154 run the model under a variety of conditions to determine the impact of NVCs from dust and sea  
155 salt (Ca, Mg, K, Na) on pH, its seasonal variability, as well as the effect of pH and temperature on  
156 nitrate partitioning.

157

## 158 **Results and discussion**

### 159 **Predicted Sulfate, ammonium & nitrate**

160 For the main inorganic aerosol species ( $\text{SO}_4^{2-}$ ,  $\text{NO}_3^-$  and  $\text{NH}_4^+$ ), CMAQ captures the  
161 observed downwards trends (Park et al. 2006, Hand et al. 2012, Blanchard et al. 2013a, b, Kim et  
162 al. 2015, Saylor et al. 2015) over the CONUS during the course of the decade (Figure S1). As  
163 expected, sulfate over the entire US drops significantly between 2001 and 2011, by about 30%,  
164 with major decreases in the Eastern US of about  $2 \mu\text{g m}^{-3}$ . Areas impacted the most by these  
165 reductions, are places of significant industrial activity or with significant coal-fired electricity  
166 generating units (EGUs), such as the Ohio River Valley, Baton Rouge in Louisiana and South  
167 Carolina. Ammonium levels remain rather constant, since ammonia saw minimal emission  
168 changes over the decade, and only experience small reductions which are a buffered response to  
169 the decrease in sulfate levels. Local reductions ( $\sim 20\%$ ) in ammonia are seen over North Carolina  
170 and Louisiana. Aerosol nitrate concentrations remain relatively constant on average over the  
171 domain, with small increases over the Eastern US. The highest levels of ammonium are observed  
172 in areas with significant livestock, such as North Carolina; sulfate concentrations are the highest



173 around the area of the Ohio River Valley, and so is nitrate due to significant NO<sub>x</sub> and SO<sub>x</sub>  
174 emissions.

### 175 **Predicted Annual & seasonal pH**

176 Figure 1 depicts the annual average pH fields over the US for 2001 and 2011 for PM<sub>2.5</sub>,  
177 with the study domain of the Eastern US outlined. Simulations show that there are noticeable  
178 differences between the two years, localized mainly in desert regions along the US-Mexico border,  
179 Southern Texas and the Eastern US. The sulfate reductions in the Eastern US, appear to have a  
180 major impact on model results, leading to significant increases of aerosol pH in the area. For 2001,  
181 the average yearly pH for the Eastern US is 1.6, consistent with recent literature and observations  
182 from the WINTER campaign (Guo et al. 2015 & 2016, Weber et al. 2016) (Figure 1a). For 2011,  
183 however, predicted pH increases to about 2.5 – almost a unit higher (Figure 1b). This trend  
184 suggests that pH will keep increasing with future sulfate reductions, something that can lead to  
185 significant increases in predicted nitrate, as well as changes in SOA chemistry which heavily  
186 depends on aerosols (Xu et al. 2015, Pye et al. 2013, Surrat et al. 2010, Eddingsaas et al. 2010),  
187 especially in the SE US.

188 Seasonal pH trends are also positive over the Eastern US, with the summertime (Figure  
189 S2f) experiencing stronger increases than in the winter (Figure S2c), being 0.5-1.5 for winter and  
190 0.5-2 for summer. Much of the seasonal variability is driven by changes in temperature and relative  
191 humidity; increased relative humidity (RH) leads to less acidic aerosol, since liquid water content  
192 and pH are inversely related (Guo et al. 2015 & 2016), while increased temperatures promote low  
193 RH and therefore more acidic aerosol. The desert areas of the Western US, Southern Texas,  
194 Florida, SW Alabama and Mississippi are the most sensitive in the wintertime (Figure S2a, b),  
195 while the Central US is mostly unaffected. During the summer, the entire Central US is much  
196 more strongly impacted, while the wintertime sensitive areas exhibit only minor pH increases  
197 (Figure S2d, e).

### 198 **Model evaluation of pH**

199 Model results for both simulation years were compared to thermodynamic analysis of  
200 measurements from three urban sites (Jefferson Street, JST; Georgia Tech, GT; Atlanta Road-  
201 Side, RS) and two rural (Yorkville, YRK; and Centerville CTR) SEARCH network sites (Guo et  
202 al. 2015, Xu et al. 2015). Measurements for the urban sites and the YRK site, were taken between  
203 May and December 2012 for the SCAPE study, while measurements from the CTR site were for





204 the SOAS campaign period (June 1<sup>st</sup> to July 15<sup>th</sup> 2013) (Guo et al. 2015, Xu et al. 2015). The three  
205 urban sites are contained within the same CMAQ grid cell. All urban sites (Figure 2a, b, c, d),  
206 exhibit an early morning/late night pH maximum, and an afternoon minimum throughout the year  
207 (Guo et al. 2015). This a combination of two factors; RH being highest during the early  
208 morning/late night, which increases water uptake and hence decreases acidity (Guo et al. 2015)  
209 (Figure S3), and the presence of crustal elements in significant quantities during that time (Figure  
210 S4). The model pH closely tracks the diurnal profile of predicted cations (Figure S4), indicating  
211 that they have an important impact on predicted pH, which, however, is not seen in the  
212 measurements (Figure 2), since they make up a much smaller percentage of observed PM<sub>2.5</sub>.  
213 Despite the presence of NVCs, the pH remains low for both simulation years but it tends to be  
214 higher in 2011, because of sulfate levels that are approximately half of those in 2001 across all  
215 sites, leading to the increased relative effect of NVCs (Weber et al. 2016). Removal of all NVCs  
216 from the thermodynamic calculations (Figure S5), allows the simulated diurnal profiles to better  
217 track the measurements. At the same time, a negative bias is introduced to the simulated pH, which  
218 is more prominent for the urban sites even after the sulfate reductions.

219 The increase in pH is not proportional to the reduction in sulfate, since aerosol responds  
220 non-linearly to such reductions, through the volatilization of ammonia (Weber et al. 2016).  
221 Depending on location, sulfate reductions range from 38 to 55%, while the corresponding pH  
222 increase is much lower, pointing to the fact that cations, although small in amount, tend to have a  
223 disproportionately strong impact on acidity. For the SOAS campaign period (Figure 2g), pH is  
224 underestimated especially for 2001. The biases follow the pattern of NVCs present, by being  
225 negatively biased until noon and positively biased for the rest of the day (Figure 2 and Figure S4).  
226 For the YRK site (Figure 2b, e), pH is overall underestimated during the winter and overestimated  
227 during the summer. Similarly to the urban sites, the predicted RH agrees well with the  
228 measurements (Figure S3), albeit with a positive afternoon bias during the summer. The diurnal  
229 profile of pH closely tracks the one of cations, further suggesting they may be directly related to  
230 the bias.

231 When evaluating the predicted pH trend for CTR, the model results exhibit a clear,  
232 increasing trend of 0.6 pH units per decade (Figure 3). This trend is inconsistent with recent  
233 thermodynamic analysis of observations suggesting a slight decrease in pH over the same time  
234 period for the SE US (Guo et al. 2015 & 2016, Weber et al. 2016). If this bias in predicted pH



235 trend continues, it can have profound implications for future regulatory modeling, since the  
236 increased pH can lead to elevated levels of model nitrate, reproducing nitrate substitution (Bauer  
237 et al. 2007, Bellouin et al. 2011, Li et al. 2014, Goto et al. 2016). Possible reasons behind this pH  
238 bias could be overestimated ammonia emissions, underestimated sulfate, or, the presence of NVCs  
239 in  $PM_{2.5}$ . The first two possibilities are unlikely, given the agreement of predicted ammonium and  
240 sulfate with previous studies (Park et al. 2006, Hand et al. 2012, Blanchard et al. 2013a, b, Kim et  
241 al. 2015, Saylor et al. 2015), and, the relative insensitivity of pH to ammonia and sulfate (Weber  
242 et al. 2016, Silvern et al. 2017). However, NVCs, if inappropriately distributed in  $PM_{2.5}$ , can exert  
243 important biases on pH (Meskhidze et al. 2003, Karydis et al. 2016, Guo et al. 2017a, Foroutan et  
244 al. 2017). Indeed, offline calculations of aerosol pH excluding the influence of NVCs mitigates  
245 most of the predicted positive trend of 0.6 pH units per decade when all the aerosol species are  
246 considered (Figure 3), while also reducing standard error. The remaining bias may arise from  
247 errors in model RH, given that it controls water uptake and drives much of the diurnal variability  
248 in pH (Guo et al. 2015). Usage of observed (instead of predicted) RH in the thermodynamic  
249 calculations, did not impact the predicted pH more than 0.1 units (Figure S6). A more thorough  
250 evaluation of the remainder of the pH bias, as well as the impact of NVCs when included in  
251 appropriate quantities, requires a far more extensive analysis of the emissions profiles – especially  
252 regarding its diurnal variability - and observational dataset than the one available for this study  
253 (Henneman et al. 2017, Guo et al. 2017).

254         The pH bias becomes negative for most of the CMAQ Eastern US when removing all  
255 NVCs from the calculations (Figure S5). This, combined with the considerable model skill for  
256 sulfate, nitrate and ammonium when compared to literature (Henneman et al. 2017) implies that  
257 pH biases are not related to errors in the major inorganic ions or biases in meteorological  
258 parameters (humidity and temperature), but rather in the NVCs which are minor contributors to  
259  $PM_{2.5}$ , hence poorly constrained. For the SEARCH sites NVCs comprise 5 to 10% of the total  
260 inorganic  $PM_{2.5}$  (Guo et al. 2015), which is significantly less than what the model predicted values  
261 that are a factor of 4 higher than the measurements. The most important result therefore is that  
262 NVCs are a considerable source of pH prediction uncertainty when not accounted for correctly  
263 (Supplementary material: The role of NVCs in  $PM_{2.5}$  pH). It should be noted that for the  
264 summertime at the CTR location, the ammonium and sulfate values are biased low in CMAQ by



265 a factor of 3 using the Weber et al. 2016 data. These biases however are consistent with literature  
266 and typical of CTMs (Henneman et al 2017).

267 The SEARCH sites have been thoroughly studied in previous literature (Guo et al, 2015 &  
268 2017a, Xu et al. 2015, Weber et al. 2016) and given the high concentrations of organic mass  
269 observed throughout the year, they present an excellent case study for the potential impact of  
270 organics on pH. Recent studies indicate that organic aerosol can have a secondary, but still  
271 quantifiable impact on aerosol pH, especially when allowed to interact with inorganics (Pye et al.  
272 2018). Most 3D models do not account for potential, non-ideal interactions between the two, in  
273 addition to not including organics in thermodynamic calculations, which, if the above statement  
274 is true, can lead to significant predictive pH errors. To investigate the role of organics on pH we  
275 used the E-AIM model (Wexler & Clegg 2002, Friese & Ebel 2010, Clegg et al. 1992)  
276 (<http://www.aim.env.uea.ac.uk/aim/aim.php>) on our model results for the SEARCH sites, to  
277 calculate partitioning with organics/inorganic interactions considered. We tested a variety of  
278 organic compounds under different scenarios to determine the potential of organics to influence  
279 pH (see SI: Organic acids and pH).

280 We find that addition of organic compounds to the model, did not have a significant impact  
281 on acidity ( $\leq 2\%$  pH deviation from the baseline value) compared to the baseline run, apart from  
282 the cases where RH was higher than 80% and the mole fraction of organic acids in the aqueous  
283 phase is greater than 25% (SI: Organic acids and pH). We conclude that the maximum impact of  
284 organics on aerosol pH can likely result from the effects of liquid-liquid phase separation (Pye et  
285 al. 2018), but of insufficient magnitude to sustain a positive aerosol pH trend as observed in our  
286 basecase simulation.

### 287 **The impact of pH biases on nitrate partitioning and “sulfate substitution”**

288 To understand the importance of pH biases on nitrate partitioning and the potential for  
289 predicting a behavior consistent with “nitrate substitution”, we express the CMAQ output in each  
290 grid cell in terms of the nitrate partitioning ratio,  $\epsilon_{NO_3} = \frac{[NO_3^-]}{[HNO_3] + [NO_3^-]}$ . It can be shown that  $\epsilon_{NO_3}$   
291 follows a simple sigmoidal curve (Meskhidze et al. 2013, Guo et al. 2016),  $\epsilon_{NO_3} = 1 - \frac{[H^+]}{[H^+] + L \cdot T \cdot \Psi}$ ,  
292 where  $L$  is the liquid water content,  $T$  is ambient temperature,  $[H^+]$  is the concentration of  $H^+$  in  
293 the aerosol aqueous phase, and  $\Psi = \frac{R \cdot [HNO_3]}{1000 \cdot P_0}$  is a constant that depends on the universal gas



294 constant ( $R$ ), the effective Henry's law constant for nitric acid in the aerosol aqueous phase ( $H_{NO_3}$ )  
295 and the ambient pressure ( $P_0$ ). Depending on the value of pH, nitrate partitioning in CMAQ can  
296 either be insensitive ( $\frac{\partial \varepsilon_{NO_3}}{\partial pH} \sim 0$ ) or sensitive ( $\frac{\partial \varepsilon_{NO_3}}{\partial pH} \sim 0.5$ ) to pH biases, depending on the month of  
297 the year considered (Figure 4). We generally find that nitrate partitioning is insensitive  
298 ( $\frac{\partial \varepsilon_{NO_3}}{\partial pH} \sim 0$ ) and heavily shifted to the gas phase ( $\varepsilon_{NO_3} \sim 0$ ) during the summer and spring (Figure  
299 4), while it becomes quite sensitive to pH errors ( $\frac{\partial \varepsilon_{NO_3}}{\partial pH} \sim 0.5$ ) in the winter and fall. For the latter  
300 case, this means that small pH perturbations in either direction can strongly affect the amount of  
301 nitrate that partitions in the aerosol phase; if the weather is sufficiently cold and  $NO_x$  emissions  
302 and pH predictions are biased sufficiently high,  $\varepsilon_{NO_3} \sim 1$ , meaning that all nitrates are partitioned  
303 to the aerosol phase and the emergence of “nitrate partitioning” behavior.

304 To exemplify the above, we determine the amount of excess nitrate from pH prediction  
305 biases as follows. Perturbing the acidity by  $\Delta pH$  from the monthly mean value along the  $\varepsilon_{NO_3}$   
306 curves (Figure 4) gives the corresponding change in the partitioning ratio ( $\Delta \varepsilon_{NO_3}$ ). Multiplying  
307  $\Delta \varepsilon_{NO_3}$  with the total nitrate ( $HNO_{3(g)} + NO_3$ ) predicted in CMAQ in each grid cell gives the total  
308 nitrate response ( $\Delta NO_3$ ) to  $\Delta pH$ . When applied to the Eastern US for  $\Delta pH = +1$  (the average pH  
309 impact of including NVCs in the  $PM_{2.5}$  calculations over the entire Eastern US) gives the  $\Delta NO_3$   
310 distributions shown in Figure 5 for the winter (Figure 5a) and the summer (Figure 5b). The  
311 predicted wintertime nitrate bias tends to be higher than in the summer, owing to the lower  
312 temperatures and higher aerosol pH levels present (which shift  $\varepsilon_{NO_3}$  towards higher values; Figure  
313 4) and the higher values of total available nitrate in the wintertime. The combination of both factors  
314 (available nitrate and high pH) is necessary for appreciable quantities of nitrate to partition, but in  
315 general the locations with a pH of between 0.5 and 1 are the most susceptible to positive pH biases,  
316 since a unit increase places nitrate partitioning into the ascending part of the S-curve (Figure 4),  
317 rapidly increasing the amount of aerosol nitrate that can form. During both seasons, areas rich in  
318 total nitrate, and a pH between 0.5 and 1.5, such as the Ohio River Valley, New York, New Jersey  
319 and South Louisiana (Figure 1, S1e, f), exhibit the largest increases in aerosol nitrate. Other  
320 locations that have low pH, and low total nitrate such as West Virginia see minimal changes. A  
321 notable exception is North Carolina which has a higher pH than the aforementioned locations -  
322 mainly due to the high  $NH_3$  emissions from livestock - which pushes the partitioning beyond the  
323 sensitive regime, where increases in pH do not drive additional nitrate in the particle phase.



324 To investigate the potential of NVCs and sulfate reductions to induce nitrate substitution,  
325 the sensitivity of the nitrate increase  $\Delta\text{NO}_3$ , to the corresponding sulfate reduction  $\Delta\text{SO}_4$ , was  
326 quantified for the Eastern US, both when NVCs are included in the calculations and when they  
327 were not (Figure 6). Over the decade, nitrate has seen increases in the Eastern US (Figure S11)  
328 ranging from 0.5 to 2.5  $\mu\text{g m}^{-3}$ , and NVCs can have a profound impact on how these increases are  
329 distributed across the domain (Figure S11a, b). In the presence of NVCs (Figure 6a), there is a 1  
330  $\mu\text{g m}^{-3}$  increase of nitrate for a sulfate reduction of the same value over the Eastern US. For this  
331 case, substitution is predicted across the entire Eastern US, with only a few gridcells in South  
332 Georgia, Mississippi and North Carolina exhibiting the opposite trend (nitrate reduction),  
333 attributed to the formation of insoluble  $\text{CaSO}_4$ , which reduces the availability of aerosol water,  
334 and in turn inhibits the formation of  $\text{NO}_3$  with the co-condensation of  $\text{NH}_3$ . When NVCs are  
335 removed (Figure 6b), the corresponding nitrate increase is much less (0-0.2  $\mu\text{g m}^{-3}$  per 1  $\mu\text{g m}^{-3}$  of  
336 sulfate), especially in the Eastern US, while substitution is still predicted in the Northern parts of  
337 the domain such as Ohio, Indiana and Michigan. The aforementioned areas, tend to have higher  
338 seasonal pH values than the SE US (Figure 1), and the removal of NVCs reduces the pH to values  
339 where nitrate partitioning is more sensitive to small pH perturbations (Figure 4), leading to a higher  
340 predicted sensitivity to sulfate reductions. This analysis suggests that nitrate substitution is of a  
341 much smaller magnitude than expected (West et al. 1999, Heald et al. 2012, Bauer et al. 2007,  
342 Bellouin et al. 2011, Li et al. 2011, Goto et al. 2016, Vayenas et al. 2005, Karydis et al. 2016), and  
343 heavily impacted by pH biases introduced from NVCs.

344 Given the importance of aerosol acidity for almost any aerosol-related process and impact,  
345 it is imperative that aerosol studies evaluate acidity inferred from thermodynamic analysis of  
346 ambient data as presented here. We demonstrate that in the case of nitrate substitution, the  
347 distribution of nonvolatile cations over particle size can have a profound impact on model  
348 behavior, and requires better constraints from emissions to observations (or at least appropriate  
349 sensitivity studies, such as those carried out here, to unravel the potential impact of nonvolatile  
350 cations). Understanding aerosol pH and the drivers thereof, is a powerful tool for evaluating model  
351 performance that has never been used before. Usage of molar ratios, ion balances and other  
352 conceptual models of aerosol acidity (Hennigan et al. 2015, Wang et al. 2016, Silvern et al. 2017)  
353 provide limited insights in aerosol pH and should be strongly avoided to limit incorrect  
354 conclusions.



## 355 **Acknowledgments**

356 We acknowledge support from the Phillips 66 company, an EPA STAR grant, Georgia Power  
357 Faculty Scholar chair funds and the European Research Council Consolidator Grant 726165 –  
358 PyroTRACH. Authors declare no conflict of interest. This work was funded, in part, by U.S.  
359 Environmental Protection Agency under grant RD834799. Its contents are solely the responsibility  
360 of the grantee and do not necessarily represent the official views of the US EPA. Further, the US  
361 EPA does not endorse the purchase of any commercial products or services mentioned in the  
362 publication. Observational data were provided by Atmospheric Research Associates.



## 363 **References**

364 Air Pollutant Emissions Trends Data, [https://www.epa.gov/air-emissions-inventories/air-](https://www.epa.gov/air-emissions-inventories/air-pollutant-emissions-trends-data)  
365 [pollutant-emissions-trends-data](https://www.epa.gov/air-emissions-inventories/air-pollutant-emissions-trends-data)

366 Bauer, S. E., Koch, D., Unger, N., Metzger, S. M., Shindell, D. T., and Streets, D. G.: Nitrate  
367 aerosols today and in 2030: a global simulation including aerosols and tropospheric ozone, Atmos.  
368 Chem. Phys., 7, 5043-5059, doi:10.5194/acp-7-5043-2007, 2007.

369 Bellouin, N., J. Rae, A. Jones, C. Johnson, J. Haywood, and O. Boucher (2011), Aerosol forcing  
370 in the Climate Model Intercomparison Project (CMIP5) simulations by HadGEM2-ES and the role  
371 of ammonium nitrate, J. Geophys. Res., 116,D20206, doi:10.1029/2011JD016074

372 Blanchard, C.L., Hidy, G.M., Tanenbaum, S., Edgerton, E.S. and Hartsell, B.E. 2013a. The  
373 Southeastern Aerosol Research and Characterization (SEARCH) study: Temporal trends in gas  
374 and PM concentrations and composition, 1999-2010. J. Air Waste Manage. Assoc., 63:247-259.

375 Blanchard, C.L., Hidy, G.M., Tanenbaum, S., Edgerton, E.S. and Hartsell, B.E. 2013b. The  
376 Southeastern Aerosol Research and Characterization (SEARCH) study: Spatial variations and  
377 chemical climatology, 1999-2010. J. Air Waste Manage. Assoc., 63:260-275.

378 Bougiatioti, A., Nikolaou, P., Stavroulas, I., Kouvarakis, G., Weber, R., Nenes, A., Kanakidou,  
379 M., and Mihalopoulos, N.: Particle water and pH in the eastern Mediterranean: source variability  
380 and implications for nutrient availability, Atmos. Chem. Phys., 16, 4579-4591, doi:10.5194/acp-  
381 16-4579-2016, 2016.

382 Byun, D. W., and K. L. Schere, 2006: Review of the governing equations, computational  
383 algorithms, and other components of the Models-3 Community Multiscale Air Quality (CMAQ)  
384 Modeling System. *Appl. Mech. Rev.*, 59, 51-77.

385 Clegg, S. L., Pitzer, K. S., and Brimblecombe, P., Thermodynamics of multicomponent, miscible,  
386 ionic solutions. II. Mixtures including unsymmetrical electrolytes. J. Phys. Chem. 96, 9470-9479,  
387 DOI: 10.1021/j100202a074, 1992



- 388 Eddingsaas, N.C, VanderVelde, D.G, and Wennberg, P.O Kinetics and Products of the Acid-  
389 Catalyzed Ring-Opening of Atmospherically Relevant Butyl Epoxy Alcohols, The Journal of  
390 Physical Chemistry A 2010 114 (31), 8106-8113, DOI: 10.1021/jp103907c  
391
- 392 Fang, T., Guo, H., Zeng, L., Verma, V., Nenes, A., Weber, R.J. (2017) Highly acidic ambient  
393 particles, soluble metals and oxidative potential: A link between sulfate and aerosol toxicity,  
394 Env.Sci.Tech., 51 (5), pp 2611–2620, doi:10.1021/acs.est.6b06151  
395
- 396 Fisher, J.A., D.J. Jacob, Q. Wang, R. Bahreini, C.C. Carouge, M.J. Cubison, J.E. Dibb, T. Diehl,  
397 J.L. Jimenez, E.M. Leibensperger, Z. Lu, M.B.J. Meinders, H.O.T. Pye, P.K. Quinn, S. Sharma,  
398 D.G. Streets, A. van Donkelaar, and R.M. Yantosca. 2011. "Sources, distribution, and acidity of  
399 sulfate-ammonium aerosol in the Arctic in winter-spring." Atmospheric Environment 45: 7301-  
400 7318.
- 401 Foroutan, H., J. Young, S. Napelenok, L. Ran, K. W. Appel, R. C. Gilliam, and J. E. Pleim (2017),  
402 Development and evaluation of a physics-based windblown dust emission scheme implemented  
403 in the CMAQ modeling system, J. Adv. Model. Earth Syst., 9, 585–608,  
404 doi:10.1002/2016MS000823.
- 405 Fountoukis, C. and Nenes, A. (2007) ISORROPIA II: A Computationally Efficient Aerosol  
406 Thermodynamic Equilibrium Model for  $K^+$ ,  $Ca^{2+}$ ,  $Mg^{2+}$ ,  $NH_4^+$ ,  $Na^+$ ,  $SO_4^{2-}$ ,  $NO_3^-$ ,  $Cl^-$ ,  $H_2O$   
407 Aerosols, Atmos.Chem.Phys., 7, 4639–4659
- 408 Friese, E. and Ebel, A., Temperature dependent thermodynamic model of the system  $H^+$  -  $NH_4^+$   
409 -  $Na^+$  -  $SO_4^{2-}$  -  $NO_3^-$  -  $Cl^-$  -  $H_2O$ . J. Phys. Chem. A, 114, 11595-11631, DOI:  
410 10.1021/jp101041j, 2010
- 411 G. Wang, R. Zhang, M. E. Gomez, L. Yang, M. Levy Zamora, M. Hu, Y. Lin, J. Peng, S. Guo, J.  
412 Meng, J. Li, C. Cheng, T. Hu, Y. Ren, Y. Wang, J. Gao, J. Cao, Z. An, W. Zhou, G. Li, J. Wang,  
413 P. Tian, W. Marrero-Ortiz, J. Secrest, Z. Du, J. Zheng, D. Shang, L. Zeng, M. Shao, W. Wang, Y.  
414 Huang, Y. Wang, Y. Zhu, Y. Li, J. Hu, B. Pan, L. Cai, Y. Cheng, Y. Ji, F. Zhang, D. Rosenfeld,  
415 P. S. Liss, R. A. Duce, C. E. Kolb, M. J. Molina, Persistent sulfate formation from London Fog to





- 416 Chinese haze. *Proc. Natl. Acad. Sci. U.S.A.* 113, 13630–13635, doi:10.1073/pnas.1616540113,  
417 2016
- 418 Ghio, A. J., Carraway, M. S. & Madden, M. C. Composition of air pollution particles and oxidative  
419 stress in cells, tissues, and living systems. *J. Toxicol. Environ. Health B* 15, 1–21 (2012).
- 420 Goto, D., Ueda, K., Ng, C.F.S., Takami, A., Ariga, T., Matsuhashi, K., Nakajima, T., Estimation  
421 of excess mortality due to long-term exposure to PM<sub>2.5</sub> in Japan using a high-resolution model  
422 for present and future scenarios. *Atmospheric Environment* 2016;140:320–332.  
423 doi:10.1016/j.atmosenv.2016.06.015
- 424 Guo, H., Liu, J., Ellis, R.A., Murphy, J.G., Froyd, K.D., Roberts, J.M., Veres, P.R., Hayes, P.L.,  
425 Jimenez, J.L., Nenes, A., and Weber, R.J. (2017) Fine particle pH and gas-particle phase  
426 partitioning of inorganic species in Pasadena, California, during the 2010 CalNex campaign,  
427 *Atmos.Chem.Phys.*, **17**, 5703–5719
- 428 Guo, H., Liu, J., Froyd, K. D., Roberts, J. M., Veres, P. R., Hayes, P. L., Jimenez, J. L., Nenes,  
429 A., and Weber, R. J.: Fine particle pH and gas–particle phase partitioning of inorganic species in  
430 Pasadena, California, during the 2010 CalNex campaign, *Atmos. Chem. Phys.*, 17, 5703-5719,  
431 doi:10.5194/acp-17-5703-2017, 2017.
- 432 Guo, H., Nenes, A., and Weber, R. J.: The underappreciated role of nonvolatile cations on aerosol  
433 ammonium-sulfate molar ratios, *Atmos. Chem. Phys. Discuss.*, [https://doi.org/10.5194/acp-2017-](https://doi.org/10.5194/acp-2017-737)  
434 737, in review, 2017
- 435 Guo, H., Sullivan, A.P., Campuzano-Jost, P., Schroder, J.C., Lopez-Hilfiger, F.D., Dibb, J.E.,  
436 Jimenez, J.L., Thornton, J.A, Brown, S.S., Nenes, A., and Weber, R.J. (2016) Fine particle pH and  
437 the partitioning of nitric acid during winter in the northeastern United States, *J.Geoph.Res.*, 121,  
438 doi:10.1002/2016JD025311
- 439 Guo, H., Weber, R.J., Nenes, A. (2017a) The sensitivity of particle pH to NH<sub>3</sub>: Can high NH<sub>3</sub>  
440 cause London Fog conditions?, *Sci.Rep.*, 7, 12109, doi:10.1038/s41598-017-11704-0
- 441 Guo, H., Xu, L., Bougiatioti, A., Cerully, K. M., Capps, S. L., Hite Jr., J. R., Carlton, A. G., Lee,  
442 S.-H., Bergin, M. H., Ng, N. L., Nenes, A., and Weber, R. J.: Fine-particle water and pH in the



- 443 southeastern United States, Atmos. Chem. Phys., 15, 5211-5228, doi:10.5194/acp-15-5211-2015,  
444 2015.
- 445 Hand, J. L., Schichtel, B. A., Malm, W. C. & Pitchford, M. L. Particulate sulfate ion concentration  
446 and SO<sub>2</sub> emission trends in the United States from the early 1990s through 2010. Atmos. Chem.  
447 Phys. 12, 10353–10365 (2012).
- 448 Hand, J. L., Schichtel, B. A., Malm, W. C., and Pitchford, M. L.: Particulate sulfate ion  
449 concentration and SO<sub>2</sub> emission trends in the United States from the early 1990s through 2010,  
450 Atmos. Chem. Phys., 12, 10353-10365, doi:10.5194/acp-12-10353-2012, 2012.
- 451 Heald, C. L. et al. Atmospheric ammonia and particulate inorganic nitrogen over the United States.  
452 Atmos. Chem. Phys. 12, 10295–10312 (2012).
- 453 Henneman, L.R.F., Liu, C., Hu, Y., Mulholland, J.A., Russell, A.G. (2017), “Air quality modeling  
454 for accountability research: Operational, dynamic, and diagnostic evaluation.”, Atm.Env., 166,  
455 551–565
- 456 Hennigan, C. J., Izumi, J., Sullivan, A. P., Weber, R. J., and Nenes, A.: A critical evaluation of  
457 proxy methods used to estimate the acidity of atmospheric particles, Atmos. Chem. Phys., 15,  
458 2775-2790, doi:10.5194/acp-15-2775-2015, 2015.
- 459 Karydis, V. A., Tsimpidi, A. P., Pozzer, A., Astitha, M., and Lelieveld, J.: Effects of mineral dust  
460 on global atmospheric nitrate concentrations, Atmos. Chem. Phys., 16, 1491-1509,  
461 doi:10.5194/acp-16-1491-2016, 2016.
- 462 Kim, P. S., Jacob, D. J., Fisher, J. A., Travis, K., Yu, K., Zhu, L., Yantosca, R. M., Sulprizio, M.  
463 P., Jimenez, J. L., Campuzano-Jost, P., Froyd, K. D., Liao, J., Hair, J. W., Fenn, M. A., Butler, C.  
464 F., Wagner, N. L., Gordon, T. D., Welti, A., Wennberg, P. O., Crounse, J. D., St. Clair, J. M.,  
465 Teng, A. P., Millet, D. B., Schwarz, J. P., Markovic, M. Z., and Perring, A. E.: Sources,  
466 seasonality, and trends of southeast US aerosol: an integrated analysis of surface, aircraft, and  
467 satellite observations with the GEOS-Chem chemical transport model, Atmos. Chem. Phys., 15,  
468 10411-10433, doi:10.5194/acp-15-10411-2015, 2015.



- 469 Laskin, A., R. C. Moffet, M. K. Gilles, J. D. Fast, R. A. Zaveri, B. B. Wang, P. Nigge, and J.  
470 Shutthanandan (2012), Tropospheric chemistry of internally mixed sea salt and organic particles:  
471 Surprising reactivity of NaCl with weak organic acids, *Journal Of Geophysical Research-*  
472 *Atmospheres*, 117, D017743.
- 473
- 474 Liu, M., Song, Y., Zhou, T., Xu, Z., Yan, C., Zheng, M., Wu, Z., Hu, M., Wu, Y., and Zhu, T.:  
475 Fine particle pH during severe haze episodes in northern China, *Geophys. Res. Lett.*, 44, 5213-  
476 5221, doi:10.1002/2017GL073210, 2017
- 477
- 478 Li, J., W.-C. Wang, H. Liao, and W. Chang. 2014. Past and future direct radiative forcing of nitrate  
479 aerosol in East Asia. *Theor. Appl. Climatol.* 1–14. doi:10.1007/s00704-014-1249-1
- 480 Liu, Y., Wu Z., Wang, Y., Xiao, Y., Gu, F., Zheng, J., Tan, T, Shang, D., Wu, Y., Zeng, L., Hu,  
481 M., Bateman, A. P., and Martin, S.T., Submicrometer Particles Are in the Liquid State during  
482 Heavy Haze Episodes in the Urban Atmosphere of Beijing, China, *Environmental Science &*  
483 *Technology Letters Article ASAP*, DOI: 10.1021/acs.estlett.7b00352, 2017
- 484 Meskhidze, N., Chameides, W. L., Nenes, A. & Chen, G. Iron mobilization in mineral dust: can  
485 anthropogenic SO<sub>2</sub> emissions affect ocean productivity? *Geophys. Res. Lett.* 30, 2085 (2003).
- 486 Park, R. J., Jacob, D. J., Kumar, N. and Yantosca, R. N.. 2006. Regional visibility statistics in the  
487 United States: Natural and transboundary pollution influences, and implications for the regional  
488 haze rule. *Atmospheric Environment* 40(28): 5405-5423,  
489 doi.org/10.1016/j.atmosenv.2006.04.059
- 490 Pinder, R. W., Adams, P. J. & Pandis, S. N. Ammonia emission controls as a cost-effective strategy  
491 for reducing atmospheric particulate matter in the eastern United States. *Environ. Sci. Technol.*  
492 41, 380–386 (2007).
- 493 Pinder, R. W., Gilliland, A. B. & Dennis, R. L. Environmental impact of atmospheric NH<sub>3</sub>  
494 emissions under present and future conditions in the eastern United States. *Geophys. Res. Lett.*  
495 35, L12808 (2008).



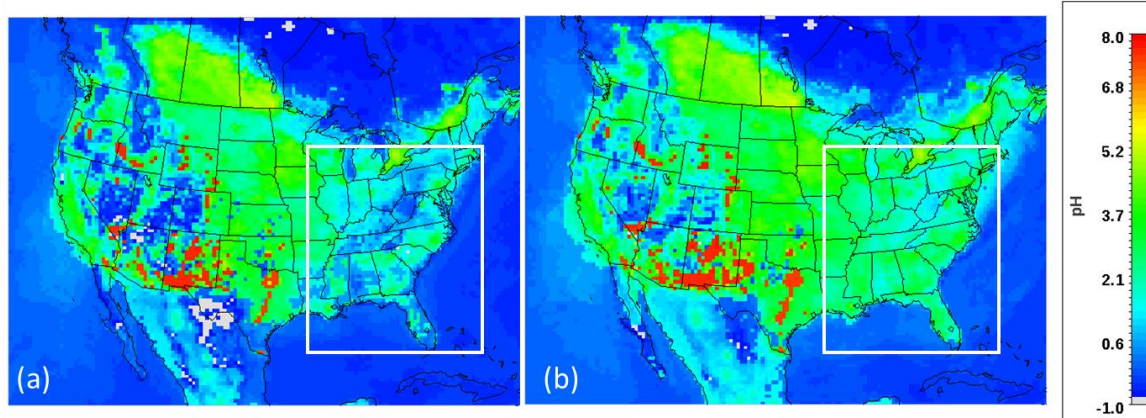
- 496 Pye, H. O. T., H. Liao, S. Wu, L. J. Mickley, D. J. Jacob, D. K. Henze, and J. H. Seinfeld (2009),  
497 Effect of changes in climate and emissions on future sulfate-nitrate-ammonium aerosol levels in  
498 the United States, *J. Geophys. Res.*, 114, D01205, doi:10.1029/2008JD010701.
- 499 Pye, H. O. T., Zuend, A., Fry, J. L., Isaacman-VanWertz, G., Capps, S. L., Appel, K. W., Foroutan,  
500 H., Xu, L., Ng, N. L., and Goldstein, A. H.: Coupling of organic and inorganic aerosol systems  
501 and the effect on gas-particle partitioning in the southeastern US, *Atmos. Chem. Phys.*, 18, 357-  
502 370, <https://doi.org/10.5194/acp-18-357-2018>, 2018.
- 503 Pye, H. O. T.; Pinder, R. W.; Piletic, I. R.; Xie, Y.; Capps, S. L.; Lin, Y.-H.<sup>S</sup>; Surratt, J. D.; Zhang,  
504 Z.; Gold, A.; Luecken, D. J.; Hutzell, W. T.; Jaoui, M.; Offenberg, J. H.; Kleindienst, T. E.;  
505 Lewandowski, M.; Edney, E. O. (2013) Epoxide Pathways Improve Model Predictions of Isoprene  
506 Markers and Reveal Key Role of Acidity in Aerosol Formation. *Environmental Science &*  
507 *Technology*, 47 (19), 11056–11064.
- 508
- 509 Saylor, R., Myles, L., Sibble, D., Caldwell, J. & Xing, J. Recent trends in gas-phase ammonia and  
510 PM<sub>2.5</sub> ammonium in the southeast United States. *J. Air Waste Manage. Assoc.* 65, 347–357  
511 (2015).
- 512 Saylor, R., Myles, L., Sibble, D., Caldwell, J. & Xing, J. Recent trends in gas-phase ammonia and  
513 PM<sub>2.5</sub> ammonium in the southeast United States. *J. Air Waste Manage. Assoc.* 65, 347–357, doi:  
514 10.1080/10962247.2014.992554, 2015
- 515 Silvern, R. F., Jacob, D. J., Kim, P. S., Marais, E. A., Turner, J. R., Campuzano-Jost, P., and  
516 Jimenez, J. L.: Inconsistency of ammonium-sulfate aerosol ratios with thermodynamic models in  
517 the eastern US: a possible role of organic aerosol, *Atmos. Chem. Phys.*, 17, 5107-5118,  
518 doi:10.5194/acp-17-5107-2017, 2017.
- 519 Song, S., Gao, M., Xu, W., Shao, J., Shi, G., Wang, S., Wang, Y., Sun, Y., and McElroy, M. B.:  
520 Fine particle pH for Beijing winter haze as inferred from different thermodynamic equilibrium  
521 models, *Atmos. Chem. Phys. Discuss.*, <https://doi.org/10.5194/acp-2018-6>, in review, 2018.



- 522 Surratt, J. D., Chan, A. W. H., Eddingsaas, N. C., Chan, M., Loza, C. L., Kwan, A. J., ... Seinfeld,  
523 J. H. (2010). Reactive intermediates revealed in secondary organic aerosol formation from  
524 isoprene. Proceedings of the National Academy of Sciences of the United States of America,  
525 107(15), 6640–6645. <http://doi.org/10.1073/pnas.0911114107>  
526
- 527 Tsimpidi, A. P., Karydis, V. A. & Pandis, S. N. Response of inorganic fine particulate matter to  
528 emission changes of sulfur dioxide and ammonia: the eastern United States as a case study. J. Air  
529 Waste Manage. Assoc. 57, 1489–1498 (2007).
- 530 Vayenas, D. V., S. Takahama, C. I. Davidson, and S. N. Pandis (2005), Simulation of the  
531 thermodynamics and removal processes in the sulfate-ammonia-nitric acid system during winter:  
532 Implications for PM<sub>2.5</sub> control strategies, J. Geophys. Res., 110, D07S14,  
533 doi:10.1029/2004JD005038.
- 534 Weber, R.J., Guo, H., Russell, A.G., Nenes, A. (2016) High aerosol acidity despite declining  
535 atmospheric sulfate concentrations over the past 15 years, Nature Geosci., doi:10.1038/ngeo2665
- 536 Weijun Li, Liang Xu, Xiaohuan Liu, Jianchao Zhang, Yangting Lin, Xiaohong Yao, Huiwang  
537 Gao, Daizhou Zhang, Jianmin Chen, Wenxing Wang, Roy M. Harrison, Xiaoye Zhang, Longyi  
538 Shao, Pingqing Fu, Athanasios Nenes, Zongbo Shi. Air pollution–aerosol interactions produce  
539 more bioavailable iron for ocean ecosystems. Science Advances, 2017; 3 (3): e1601749 DOI:  
540 10.1126/sciadv.1601749
- 541 West, J. J., Ansari, A. S. & Pandis, S. N. Marginal PM<sub>2.5</sub>: nonlinear aerosol mass response to  
542 sulfate reductions in the eastern United States. J. Air Waste Manage. Assoc. 49, 1415–1424  
543 (1999).
- 544 Wexler, A. S., and S. L. Clegg, Atmospheric aerosol models for systems including the ions H<sup>+</sup>,  
545 NH<sub>4</sub><sup>+</sup>, Na<sup>+</sup>, SO<sub>4</sub><sup>2-</sup>, NO<sub>3</sub><sup>-</sup>, Cl<sup>-</sup>, Br<sup>-</sup>, and H<sub>2</sub>O, J. Geophys. Res., 107(D14), DOI:  
546 10.1029/2001JD000451, 2002, <http://www.aim.env.uea.ac.uk/aim/aim.php>
- 547 Xu, L.; Guo, H.; Boyd, C.; Klein, M.; Bougiatioti, A.; Cerully, K.; Hite, J.; Isaacman-VanWertz,  
548 G.; Kreisberg, N. M.; Knote, C.; Olson, K.; Koss, A.; Goldstein, A.; Hering, S. V.; de Gouw, J.;  
549 Baumann, K.; Lee, S. H.; Nenes, A.; Weber, R. J.; Ng, N. L. Effects of anthropogenic emissions



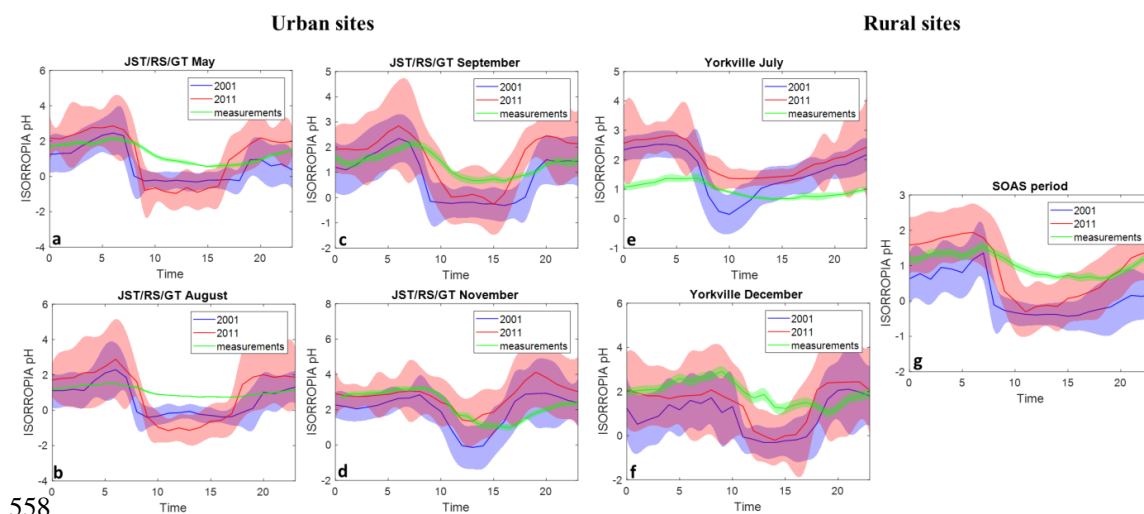
550 on aerosol formation from isoprene and monoterpenes in the southeastern United States. Proc.  
551 Natl. Acad. Sci. U. S. A. 2014, 112 (1), 37–42.  
552



553

554 **Figure 1** - Annual averaged  $PM_{2.5}$  pH over CONUS for (a) 2001 and (b) 2011, calculated offline  
555 using ISORROPIA, using the annual averaged CMAQ concentration fields. The white outline  
556 specifies the Eastern US domain used for further analysis.

557



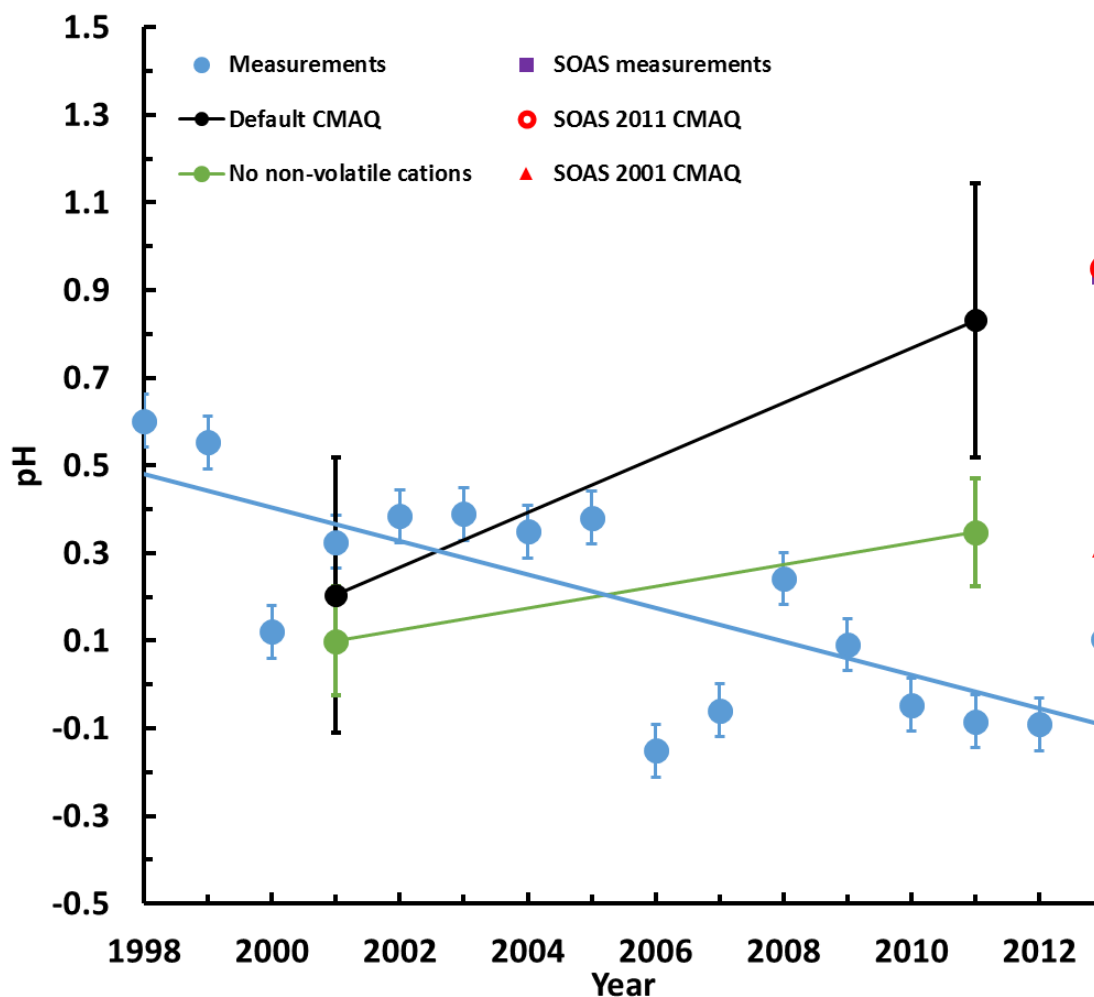
558

559 **Figure 2** - pH diurnal profiles for May (a), August (b), September (c) and November (d)  
560 JST/RS/GT, July (e) and December (f) at YRK and for the SOAS campaign period (g). Blue and  
561 red lines are the CMAQ predicted pH for 2001 and 2011 respectively, while the shaded areas are  
562 one model standard deviation. The green line represents the pH calculated through the





563 thermodynamic analysis of the measurements and the shaded area is standard

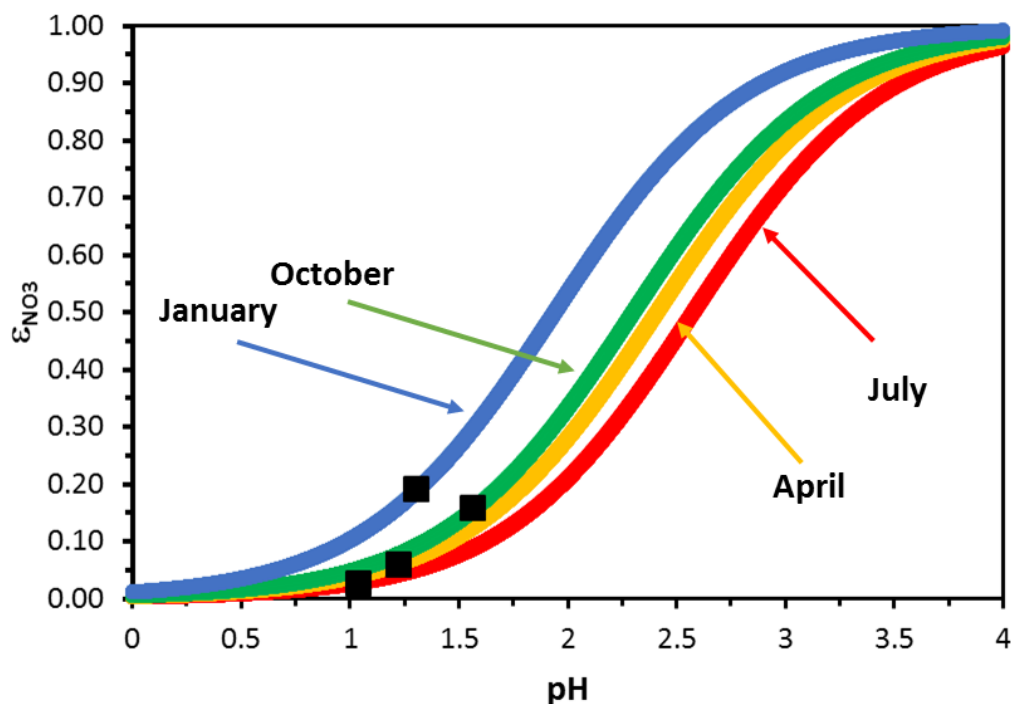


564

565 **Figure 3** – Decadal pH trends from the thermodynamic analysis of the measurements from Weber  
566 et al. 2016 (blue line), default CMAQ (black line) and CMAQ results without crustal elements  
567 (green line). Also shown, is the pH for the SOAS campaign, and for the CMAQ predicted pH for  
568 June 1<sup>st</sup>-July 15<sup>th</sup> 2001 and 2011. CMAQ exhibits a clear positive trend, with pH increasing  
569 throughout the decade, both due to sulfate reductions and the increasingly important role of NVCs.  
570 Standard error is also plotted for all data points.

571

572



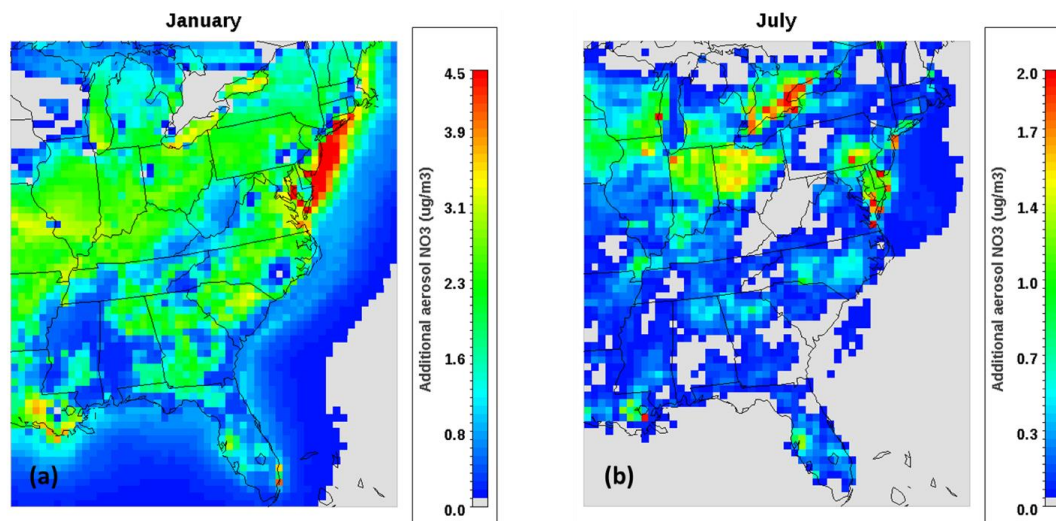
573

574 **Figure 4** - CMAQ-derived nitrate partitioning ratio for the E.US and select months of 2001. The  
575 black squares denote the average pH values for each month. Note the insensitivity of nitrate  
576 partitioning to pH biases in the summer for pH values of less than 1 ( $\frac{\partial \epsilon_{NO_3}}{\partial pH} \sim 0$ ), which is not the case  
577 for colder months.

578



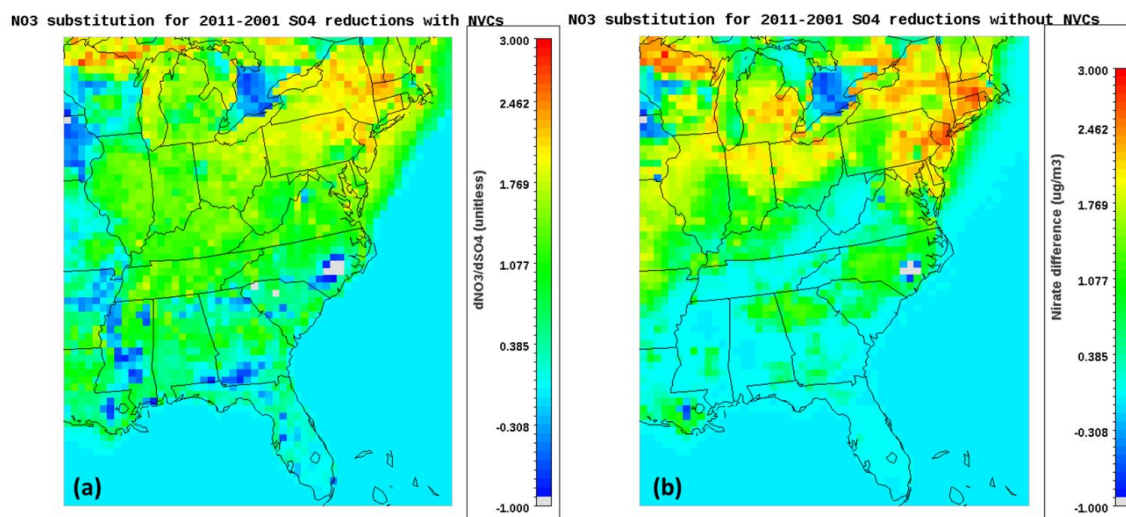
579



580

581 **Figure 5** - Increase in aerosol nitrate corresponding to a one-unit positive in pH for a) winter and  
 582 b) summer. Emissions for 2011 are assumed, but to account for pH prediction biases from NVCs,  
 583 they are removed from the thermodynamic calculations. Plots are on different scales due to the  
 584 large differences in predicted nitrate increases.

585



586 **Figure 6** – CMAQ predicted nitrate substitution  $\left(\frac{NO_3^{2011}-NO_3^{2001}}{SO_4^{2001}-SO_4^{2011}}\right)$  over the decade, when NVCs  
 587 are accounted for (a), and when they are removed from the thermodynamic calculations (b).